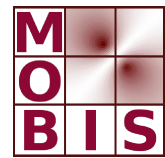
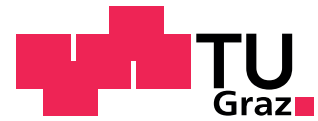




SpezialForschungsBereich F 32



Karl-Franzens Universität Graz  
Technische Universität Graz  
Medizinische Universität Graz



# A TGV Regularized Wavelet Based Zooming Model

K. Bredies      M. Holler

SFB-Report No. 2013-005

March 2013

A-8010 GRAZ, HEINRICHSTRASSE 36, AUSTRIA

Supported by the  
Austrian Science Fund (FWF)

**FWF** Der Wissenschaftsfonds.

SFB sponsors:

- **Austrian Science Fund (FWF)**
- **University of Graz**
- **Graz University of Technology**
- **Medical University of Graz**
- **Government of Styria**
- **City of Graz**



# A TGV Regularized Wavelet Based Zooming Model

Kristian Bredies and Martin Holler

Institute of Mathematics and Scientific Computing, University of Graz,  
Heinrichstraße 36, A-8010 Graz, Austria

**Abstract.** We propose and state a novel scheme for image magnification. It is formulated as a minimization problem which incorporates a data fidelity and a regularization term. Data fidelity is modeled using a wavelet transformation operator while the *Total Generalized Variation* functional of second order is applied for regularization. Well-posedness is obtained in a function space setting and an efficient numerical algorithm is developed. Numerical experiments confirm a high quality of the magnified images. In particular, with an appropriate choice of wavelets, geometrical information is preserved.

## 1 Introduction

We consider the problem of obtaining a high resolution image from low resolution data. This can be seen as an inverse problem, where the objective is the inversion of a downsampling operator denoted by  $A$ . This problem is ill-posed since the kernel of  $A$  is large. A standard technique to obtain well-posedness is to apply Tikhonov regularization with a regularization functional that we denote by  $G$ . The task of reconstructing a high resolution image  $\hat{u}$  that fits to given low resolution image data  $d$  can then be realized by solving

$$\min_u G(u) + \mathcal{I}_{U_D}(u) \Leftrightarrow \min_{Au=d} G(u),$$

where  $U_D = \{u \mid Au = d\}$  and  $\mathcal{I}_{U_D}$  is the convex indicator function w.r.t.  $U_D$ . In order to achieve a natural-looking result, we have to make appropriate choices for the downsampling operator  $A$  and the regularization term  $G$ , both having strong influence on the obtained reconstruction quality.

*Downsampling* The first question is how to describe the downsampling procedure, i.e. the process of obtaining discrete pixel values from an image  $u$  defined, for instance, on the unit square. The multiresolution approach of wavelet bases provides a framework to describe downsampling procedures: In a simple, one dimensional setting, given orthogonal scaling and wavelet functions  $(\phi_{j,k})_{j,k \in \mathbb{Z}}$  and  $(\psi_{j,k})_{j,k \in \mathbb{Z}}$ , respectively, any signal  $u \in L^2(\mathbb{R})$  can be fully described by the  $L^2$ - inner products

$$(u, \phi_{R,k})_2, \quad (u, \psi_{j,k})_2, \quad \text{for } j, k \in \mathbb{Z}, j \leq R,$$

for any  $R \in \mathbb{Z}$  fixed. In this context, the inner products  $((u, \phi_{R,k})_2)_{k \in \mathbb{Z}}$ , can be interpreted to be the values of the signal  $u$  at resolution  $R$ , while the inner products  $((u, \psi_{j,k})_2)_{j \leq R, k \in \mathbb{Z}}$  contain all remaining detail information. Thus, the mapping that asserts to any given signal  $u$  the inner products  $((u, \phi_{R,k})_2)_{k \in \mathbb{Z}}$  can be seen as a subsampling operation to a resolution  $R$ . Since this multiresolution framework can be considered for any choice of wavelet basis, even for non-orthogonal Riesz bases, it allows a general approach to a downsampling operator for the zooming problem. Thus, given the multiresolution framework of any wavelet basis and fixed a resolution level  $R \in \mathbb{Z}$ , we define the linear downsampling operator to be

$$u \mapsto ((u, \phi_{R,k})_2)_{k \in \mathbb{Z}}.$$

*Regularization* The second choice is the regularization term. Naturally, this choice should reflect typical properties of realistic images, in particular allow jump discontinuities. We will use the *Total Generalized Variation (TGV)* functional of second order for regularization (see [3]). As the well known *Total Variation* functional, it allows jump discontinuities in the continuous setting, but is also aware of second-order features. As a result, it favors piecewise linear reconstructions, yielding an improved image quality (see for example [1–3]).

Thus, given the scaling functions  $(\phi_{R,k})_{k \in \mathbb{Z}}$ , in order to obtain a high resolution image from low resolution data  $d = (d_k)_{k \in \mathbb{Z}}$ , our aim is to solve

$$\min_u \text{TGV}_\alpha^2(u) + \mathcal{I}_{U_D}(u) \tag{1}$$

where

$$U_D = \{u \mid (u, \phi_{R,k})_2 = d_k \text{ for all } k \in \mathbb{Z}\}. \tag{2}$$

We ask for the readers patience until Section 2 for a definition of  $\text{TGV}_\alpha^2$ .

The idea of image zooming by interpolating wavelet coefficients is not new; we refer to [12] and the references therein for an overview. However, the crucial point of these approaches is how to obtain the missing detail coefficients. In contrast to the methods in [12], we propose to use a variational technique, in particular TGV regularization, to resolve this issue.

Variational methods have already been applied for the related problem of recovering wavelet data of JPEG 2000 compressed images, missing due to transmission errors: We refer to [15] for a nonlocal TV regularized model and the references therein. Last but not least we refer to [6, 13] for TV regularized zooming methods.

TGV Regularization has already been applied by the authors in [2] to a similar problem setting in the context of JPEG decompression. Even though the setting of [2] also allows for TGV regularized zooming, the analytical as well as numerical framework relies on orthonormal basis transforms and thus is not applicable for general wavelet transforms.

The present paper is structured as follows: In the next section we rigorously state the minimization problem (1) in a function space setting and show existence of a solution. In the third section, we provide an algorithm for the numerical

solution and in the last section we present numerical results that illustrate the good reconstruction quality of our approach.

## 2 Problem statement

Let  $\Omega \subset \mathbb{R}^2$  be a bounded Lipschitz domain. The total generalized variation functional, as introduced in [3], can be defined for arbitrary order  $K \in \mathbb{N}$  and is a non-trivial generalization of the total variation (TV) functional in the sense that it is equivalent to the TV functional for  $K = 1$ .

We are interested in the second order TGV functional, which can be defined, for  $\alpha \in (\mathbb{R}^+)^2$ ,  $u \in L^1_{\text{loc}}(\Omega)$ , as

$$\text{TGV}_\alpha^2(u) = \sup \left\{ \int_\Omega u \operatorname{div}^2 v \, dx \mid v \in \mathcal{C}_c^2, \|v\|_\infty \leq \alpha_0, \|\operatorname{div} v\|_\infty \leq \alpha_1 \right\}. \quad (3)$$

It has been shown in [5], that  $\text{TGV}_\alpha^2$  can equivalently be written as

$$\text{TGV}_\alpha^2(u) = \min_{v \in \text{BD}(\Omega, \mathbb{R}^2)} (\alpha_1 \|Du - v\|_{\mathcal{M}} + \alpha_0 \|\mathcal{E}v\|_{\mathcal{M}}), \quad (4)$$

with  $D$  and  $\mathcal{E}$  being the weak gradient and the weak symmetrized gradient, respectively,  $\text{BD}(\Omega, \mathbb{R}^2)$  being the set of  $L^1(\Omega, \mathbb{R}^2)$  functions  $v$  such that  $\mathcal{E}v$  is a finite Radon measure and  $\|\cdot\|_{\mathcal{M}}$  being the Radon norm. This gives insight to the structure of  $\text{TGV}_\alpha^2$ : Its evaluation can be interpreted as local optimal balancing between the first and the second order derivative of  $u$ , penalizing jumps in the original function as well as the derivative, but not penalizing linear ascent. Thus one would expect  $\text{TGV}_\alpha^2$  not to suffer from first order staircasing effects, as has been confirmed in [4] in a particular setting.

The following proposition summarizes analytical properties of the  $\text{TGV}_\alpha^2$  functional [3, 4].

**Proposition 21** *Let  $\Omega \subset \mathbb{R}^2$  be a bounded Lipschitz domain and  $\alpha \in (\mathbb{R}^+)^2$ .*

- $\text{TGV}_\alpha^2$  is proper, convex and lower semi-continuous as function from  $L^1(\Omega)$  to  $\mathbb{R} \cup \{\infty\}$ .
- $\text{TGV}_\alpha^2$  and  $\text{TGV}_{\tilde{\alpha}}^2$  are equivalent for any  $\tilde{\alpha} \in (\mathbb{R}^+)^2$ .
- There exist constants  $c, C > 0$  such that

$$c(\|u\|_1 + \text{TV}(u)) \leq \|u\|_1 + \text{TGV}_\alpha^2(u) \leq C(\|u\|_1 + \text{TV}(u))$$

for any  $u \in L^1(\Omega)$ .

- There exists a constant  $C > 0$  such that

$$\|u - P_1(u)\|_2 \leq C \text{TGV}_\alpha^2(u)$$

for any  $u \in L^1(\Omega)$ , where  $P_1$  is a linear projection to the space of affine functions.

These properties will allow us to obtain existence of a solution for the  $\text{TGV}_\alpha^2$  regularized wavelet based zooming problem.

For data fidelity, in particular for the subsampling operation, we want to use an arbitrary Riesz basis [14, Section 1.8] related to a wavelet based multiresolution framework: Given a function  $\phi \in L^2(\mathbb{R})$ , the scaling function, it has been shown in [8] that, under certain assumptions, one can define a corresponding mother wavelet function  $\psi \in L^2(\mathbb{R})$ . With that, a Riesz basis of  $L^2(\mathbb{R})$  can be constructed from translations and dilatations of the scaling function and the mother wavelet. We will in particular only consider scaling functions  $\phi$  having compact support, which then results in compactly supported basis elements.

This basis can then be used to first construct a Riesz basis of  $L^2((0, 1))$  by applying a folding technique [9, Section 2] that corresponds to natural boundary extension. Subsequently, a Riesz basis of  $L^2((0, 1) \times (0, 1))$  can be obtained using tensor products of the  $L^2((0, 1))$ -basis elements, similar as in [10, Section 10.1]. Thus, given any suitable  $\phi \in L^2(\mathbb{R})$ , and fixed a resolution level  $R \in \mathbb{Z}$ , we can construct a Riesz basis of  $L^2((0, 1) \times (0, 1))$  that will be denoted by

$$(\phi_{R,\mathbf{k}})_{\mathbf{k} \in M_R} \quad (\psi_{j,\mathbf{k}})_{j \leq R, \mathbf{k} \in L_j}, \quad (5)$$

with  $M_R, (L_j)_{j \leq R}$  finite index sets in  $\mathbb{Z}^2$ . Note that finiteness of those index sets is due to the folding and that  $(\psi_{j,\mathbf{k}})_{j \leq R, \mathbf{k} \in L_j}$  has infinitely many elements since  $j$  is an arbitrary integer less or equal to  $R$ .

For any Riesz basis, there also exists a dual Riesz basis [14, Chapter 1], which in this setting again results from translations and dilatations of functions  $\tilde{\phi}$  and  $\tilde{\psi}$  [8, 9], and the dual basis to (5) can be denoted by

$$(\tilde{\phi}_{R,\mathbf{k}})_{\mathbf{k} \in M_R} \quad (\tilde{\psi}_{j,\mathbf{k}})_{j \leq R, \mathbf{k} \in L_j}. \quad (6)$$

Further, any  $u \in L^2(\Omega)$ , with  $\Omega := (0, 1) \times (0, 1)$ , can be written as

$$\begin{aligned} u &= \sum_{\mathbf{k} \in M_R} (u, \tilde{\phi}_{R,\mathbf{k}})_2 \phi_{R,\mathbf{k}} + \sum_{j \leq R, \mathbf{k} \in L_j} (u, \tilde{\psi}_{j,\mathbf{k}})_2 \psi_{j,\mathbf{k}} \\ &= \sum_{\mathbf{k} \in M_R} (u, \phi_{R,\mathbf{k}})_2 \tilde{\phi}_{R,\mathbf{k}} + \sum_{j \leq R, \mathbf{k} \in L_j} (u, \psi_{j,\mathbf{k}})_2 \tilde{\psi}_{j,\mathbf{k}}. \end{aligned}$$

Now assuming a low resolution image  $u_0 \in \text{span}\{\tilde{\phi}_{R,\mathbf{k}} | \mathbf{k} \in M_R\}$  to be given by  $((u_0, \phi_{R,\mathbf{k}})_2)_{\mathbf{k} \in M_R}$ , our aim is to reconstruct a high resolution image

$$u \in L^2(\Omega) = \text{span}\left(\{\tilde{\phi}_{R,\mathbf{k}} | \mathbf{k} \in M_R\} \cup \{\tilde{\psi}_{j,\mathbf{k}} | j \leq R, \mathbf{k} \in L_j\}\right)$$

such that  $(u, \phi_{R,\mathbf{k}})_2 = (u_0, \phi_{R,\mathbf{k}})_2$  for all  $\mathbf{k} \in M_R$ . This amounts to solve

$$\min_{u \in L^2(\Omega)} \text{TGV}_\alpha^2(u) + \mathcal{I}_{U_D}(u), \quad (7)$$

where  $U_D = \{u \in L^2(\Omega) | (u, \phi_{R,\mathbf{k}})_2 = (u_0, \phi_{R,\mathbf{k}})_2 \text{ for all } \mathbf{k} \in M_R\}$ . In order to obtain well posedness of (7), we need the additional assumption that the dual

scaling basis  $(\tilde{\phi}_{R,\mathbf{k}})_{\mathbf{k} \in M_R}$  is contained in  $\text{BV}(\Omega)$  and that at least three of the functions  $(\phi_{R,\mathbf{k}})_{\mathbf{k} \in M_R}$  have support contained in  $\Omega$ .

These assumptions, however, are quite weak: By using the  $\text{TGV}_\alpha^2$  functional as regularization we implicitly assume that images are contained in  $\text{BV}(\Omega)$ , thus it is natural to require this weak form of regularity also for the basis functions of the low resolution images. Also, one of the main points for wavelet bases to be practicable is that they are compactly supported. In that case, the support assumption is satisfied if the resolution  $R$  is sufficiently fine, i.e. if the discrete image contains sufficiently many pixels. Using the Haar wavelet, for example, this requires the image to have more than  $2 \times 2$  pixels.

The support assumption is necessary due to the folding: In order to ensure that some folded functions  $(\phi_{R,\mathbf{k}})_{\mathbf{k} \in M_R}$  are indeed translations of each other, their support must not intersect the boundary.

**Proposition 22** *Fixed any  $R \in \mathbb{Z}$ , assume that the functions  $(\tilde{\phi}_{R,\mathbf{k}})_{\mathbf{k} \in M_R}$  are contained in  $\text{BV}(\Omega)$ . Further, assume that there exists  $\mathbf{k}_0 = (k_0^1, k_0^2) \in M_R$  such that*

$$\text{supp}(\phi_{R,k_0^1+l_1,k_0^2+l_2}) \subset \Omega$$

for all  $(l_1, l_2) \in \{(0, 0), (1, 0), (0, 1)\}$ . Then, the minimization problem (7) admits a solution  $\hat{u} \in \text{BV}(\Omega)$ .

*Proof (Sketch of proof).* We have that  $u_0 \in \text{BV}(\Omega) \cap U_D$  by being a finite linear combination of  $\text{BV}(\Omega)$  functions, thus the objective functional of (7) is proper (see Proposition 21) and it is non-negative. Taking  $(u_n)_{n \in \mathbb{N}}$  to be a minimizing sequence, by the estimate on  $\|u_n - P_1(u_n)\|_2$  as in Proposition 21, it suffices to bound  $(\|P_1(u_n)\|_2)_{n \in \mathbb{N}}$  in order to bound  $(\|u_n\|_2)_{n \in \mathbb{N}}$ . We denote

$$(P_1(u_n))(x, y) = c_n^1 + c_n^2 x + c_n^3 y.$$

Now due to the support restriction we get that

$$\phi_{R,k_0^1+1,k_0^2}(x, y) = \phi_{R,k_0^1,k_0^2}(x-1, y) \quad \text{and} \quad \phi_{R,k_0^1,k_0^2+1}(x, y) = \phi_{R,k_0^1,k_0^2}(x, y-1).$$

Thus, denoting by  $\mathbf{1}, \mathbf{x}, \mathbf{y}$  the functions mapping each  $(x, y)$  to  $1, x, y$ , respectively, it follows

$$\begin{aligned} (P_1(u_n), \phi_{R,k_0^1,k_0^2})_2 &= c_n^1(\phi_{R,\mathbf{k}_0}, \mathbf{1})_2 + c_n^2(\phi_{R,\mathbf{k}_0}, \mathbf{x})_2 + c_n^3(\phi_{R,\mathbf{k}_0}, \mathbf{y})_2, \\ (P_1(u_n), \phi_{R,k_0^1+1,k_0^2})_2 &= (c_n^1 + c_n^2)(\phi_{R,\mathbf{k}_0}, \mathbf{1})_2 + c_n^2(\phi_{R,\mathbf{k}_0}, \mathbf{x})_2 + c_n^3(\phi_{R,\mathbf{k}_0}, \mathbf{y})_2, \\ (P_1(u_n), \phi_{R,k_0^1,k_0^2+1})_2 &= (c_n^1 + c_n^3)(\phi_{R,\mathbf{k}_0}, \mathbf{1})_2 + c_n^2(\phi_{R,\mathbf{k}_0}, \mathbf{x})_2 + c_n^3(\phi_{R,\mathbf{k}_0}, \mathbf{y})_2. \end{aligned}$$

Now, by  $(u_0, \phi_{R,\mathbf{k}}) = (u_n, \phi_{R,\mathbf{k}})$  for all  $\mathbf{k} \in M_R$  and  $n \in \mathbb{N}$ , and by boundedness of  $(\|u_n - P_1(u_n)\|_2)_{n \in \mathbb{N}}$ , the left hand sides of these equations are bounded. An easy calculation hence yields boundedness of  $(c_n^1, c_n^2, c_n^3)_{n \in \mathbb{N}}$  and, consequently, boundedness of  $(\|P_1(u_n)\|_2)_{n \in \mathbb{N}}$ . Thus  $\|u_n\|_2$  is bounded and, since bounded sets in  $L^2(\Omega)$  are relatively weakly compact, there exists a subsequence, converging to some  $\hat{u} \in L^2(\Omega)$  weakly in  $L^2(\Omega)$ . By convexity and norm closedness of  $U_D$  we get weak closedness, thus  $\hat{u} \in U_D$ , and by  $L^1$  lower semi-continuity and convexity of  $\text{TGV}_\alpha^2$  that  $\hat{u}$  is indeed a minimizer of (7).

Within the assumptions of Proposition 22 we can now freely choose a scaling function  $\phi$  and the resulting multiresolution framework. In the following we will briefly discuss some possible choices and their interpretation.

*Choice of scaling and wavelet functions* For a simple interpretation of the choice of a scaling- and wavelet function, we will, for the rest of this section, go back to the unconstrained, one dimensional setting. Assuming a discrete signal to be given by  $((u, \phi_{R,k})_2)_{k \in \mathbb{Z}}$ , for fixed  $R \in \mathbb{Z}$ , i.e.  $u \in \text{span}\{\tilde{\phi}_{R,k} \mid k \in \mathbb{Z}\} \subset L^2(\mathbb{R})$ , its projection onto the smaller, low resolution subspace  $\text{span}\{\tilde{\phi}_{R+1,k} \mid k \in \mathbb{Z}\}$  is described by

$$(u, \phi_{R+1,k})_2 = \sum_{l \in \mathbb{Z}} h_l (u, \phi_{R,l+2k})_2, \quad k \in \mathbb{N}, \quad (8)$$

i.e. linear filtering followed by subsampling, where the filters can be constructed from  $\phi$  (see [8]). Similar, obtaining a higher resolution representation from low resolution data amounts to set

$$(u, \phi_{R,m})_2 = \sum_{k \in \mathbb{Z}} \left[ \tilde{h}_{m-2k} (u, \phi_{R+1,k})_2 + (-1)^{m-2k} \tilde{h}_{1-(m-2k)} (u, \psi_{R+1,k})_2 \right],$$

i.e. upsampling followed by linear filtering, where again the filters can be constructed from  $\phi$ . Not knowing the coefficients  $(u, \psi_{R+1,k})_2$ , a straightforward upsampling can be obtained by assuming them to be zero, thus

$$(u, \phi_{R,m})_2 \approx \sum_{k \in \mathbb{Z}} \tilde{h}_{m-2k} (u, \phi_{R+1,k})_2. \quad (9)$$

We will now interpret this approximations for different choices of scaling functions.

*Haar wavelet:* A first, intuitive choice of one dimensional scaling function, from which the two dimensional scaling and wavelet functions can be obtained, would be to define

$$\tilde{\phi}(x) = \chi_{[0,1)}(x).$$

This yields the well known Haar wavelet (cf. [8, Section 6.A]), and the filters associated with  $\phi$  and  $\tilde{\phi}$  are given by

$$2^{-1/2} h_0 = 2^{-1/2} \tilde{h}_0 = \frac{1}{2}, \quad 2^{-1/2} h_1 = 2^{-1/2} \tilde{h}_1 = \frac{1}{2}.$$

Thus, the down- and upsampling as in Equations (8),(9) is given by

$$2^{-1/2} (u, \phi_{R+1,k})_2 = \frac{1}{2} [(u, \phi_{R,2k})_2 + (u, \phi_{R,1+2k})_2],$$

$$2^{-1/2} (u, \phi_{R,2l})_2 \approx \frac{1}{2} (u, \phi_{R+1,l})_2, \quad 2^{-1/2} (u, \phi_{R,2l+1})_2 \approx \frac{1}{2} (u, \phi_{R+1,l})_2.$$

This corresponds to downsampling by averaging and upsampling by pixel repetition.

*LeGall wavelet:* Another choice is to define

$$\tilde{\phi}(x) = (1+x)\chi_{[-1,0)}(x) + (1-x)\chi_{[0,1)}(x)$$

i.e. a piecewise linear scaling function. This yields the LeGall wavelet used for lossless coding in JPEG 2000 compression (cf. [8, Section 6.A]), and the filters associated with  $\phi$  and  $\tilde{\phi}$  are given by

$$2^{-1/2}\tilde{h}_0 = \frac{1}{2}, 2^{-1/2}\tilde{h}_{\pm 1} = \frac{1}{4}, 2^{-1/2}h_0 = \frac{3}{4}, 2^{-1/2}h_{\pm 1} = \frac{1}{4}, 2^{-1/2}h_{\pm 2} = -\frac{1}{8}.$$

The down- and upsampling as in Equations (8),(9) can then be given by

$$2^{-1/2}(u, \phi_{R+1,k})_2 = \frac{3}{4}(u, \phi_{R,2k})_2 + \frac{1}{4} \sum_{l=\pm 1} (u, \phi_{R,2k+l})_2 - \frac{1}{8} \sum_{l=\pm 2} (u, \phi_{R,2k+l})_2,$$

$$2^{-1/2}(u, \phi_{R,2l})_2 \approx \frac{1}{2}(u, \phi_{R+1,l})_2,$$

$$2^{-1/2}(u, \phi_{R,2l+1})_2 \approx \frac{1}{4}(u, \phi_{R+1,l-1})_2 + \frac{1}{4}(u, \phi_{R+1,l})_2.$$

This corresponds to upsampling by linear interpolation.

*CDF 9/7 wavelet:* At last we will also use the CDF 9/7 wavelets, which are the basis for lossy JPEG 2000 coding, and whose filters can be found in [8, Table 6.2]. Again, the upsampling process can be seen as linear filtering, but we do not have a direct interpretation.

### 3 Discretization

For the discrete setting, we define  $U = \mathbb{R}^{N \times N}$ ,  $N \in \mathbb{N}$ , to be the space of discrete, high resolution images, equipped with

$$\|u\|_U^2 = \sum_{0 \leq i,j < N} u_{i,j}^2.$$

Given scaling functions  $(\phi_{j,\mathbf{k}})_{j \in \mathbb{Z}, \mathbf{k} \in \mathbb{N}_0^2}$  and the corresponding wavelet functions  $(\psi_{j,\mathbf{k}})_{j \in \mathbb{Z}, \mathbf{k} \in \mathbb{N}_0^2}$  with their duals  $(\tilde{\phi}_{j,\mathbf{k}})_{j \in \mathbb{Z}, \mathbf{k} \in \mathbb{N}_0^2}$  and  $(\tilde{\psi}_{j,\mathbf{k}})_{j \in \mathbb{Z}, \mathbf{k} \in \mathbb{N}_0^2}$ , we assume that the pixels of any discrete image  $u \in U$  can be described by the coefficients

$$(u, \phi_{0,\mathbf{k}})_2, \quad 0 \leq \mathbf{k} < N,$$

where  $0 \leq \mathbf{k} < N$  is meant component wise. For  $R \in \mathbb{N}$ , a low resolution image  $\tilde{v}_0 \in \mathbb{R}^{(2^{-R}N) \times (2^{-R}N)}$  can then be obtained from  $v_0 \in U$  by applying a discrete wavelet transform operator  $W : U \rightarrow U$  and taking

$$(Wv_0)_{\mathbf{k}} = (v_0, \phi_{R,\mathbf{k}})_2, \quad 0 \leq \mathbf{k} < 2^{-R}N,$$

to be its pixel values. The other way around, assuming  $\tilde{v}_0 \in \mathbb{R}^{(2^{-R}N) \times (2^{-R}N)}$  to be given, one aims to find  $v_0 \in U$  such that

$$(Wv_0)_{\mathbf{k}} = (\tilde{v}_0)_{\mathbf{k}}, \quad 0 \leq \mathbf{k} < 2^{-R}N,$$

i.e. an image  $v_0 \in U$  such that  $v_0$  yields  $\tilde{v}_0$  when subsampled using the wavelet transform.

Thus, given a discrete image  $u_0 \in \mathbb{R}^{(2^{-R}N) \times (2^{-R}N)}$  with  $R \in \mathbb{N}$  and a wavelet transform operator  $W$  corresponding to scaling functions  $(\tilde{\phi}_{R,\mathbf{k}})_{\mathbf{k} \in \mathbb{N}_0^2}$ , the discrete data set  $U_D$  can be written as

$$U_D = \{u \in U \mid (Wu)_{\mathbf{k}} = (u_0)_{\mathbf{k}}, \text{ for all } 0 \leq \mathbf{k} < 2^{-R}N\}. \quad (10)$$

To define the  $\text{TGV}_\alpha^2$  functional we need the operators  $\nabla : U \rightarrow U^2$ ,  $\mathcal{E} = \frac{1}{2}(J + J^T) : U^2 \rightarrow U^3$ , where  $\nabla$  and  $J$  are discrete gradient and Jacobian operators, using forward and backward differences, respectively. Motivated by the representation (4) we then define the discrete  $\text{TGV}_\alpha^2$  functional  $\text{TGV}_\alpha^2 : U \rightarrow \mathbb{R}$  as

$$\text{TGV}_\alpha^2(u) = \min_{v \in U^2} \alpha_1 \|\nabla u - v\|_1 + \alpha_0 \|\mathcal{E}v\|_1, \quad (11)$$

with

$$\|v\|_1 = \sum_{i,j} \sqrt{(v_{i,j}^1)^2 + (v_{i,j}^2)^2}, \quad \|w\|_1 = \sum_{i,j} \sqrt{(w_{i,j}^1)^2 + (w_{i,j}^2)^2 + 2(w_{i,j}^3)^2}.$$

Note that we abuse notation by using the same symbol for a  $L^1$  type norm on both  $U^2$  and  $U^3$ . Defining the spaces  $X = U^3$  and  $Z = U^6$ , the discrete minimization problem for wavelet based zooming can be written as

$$\min_{x \in X} F(Kx) \quad (12)$$

with  $F : Z \rightarrow \mathbb{R} \cup \{\infty\}$ ,  $K : X \rightarrow Z$ , defined by

$$F(v, w, r) = \alpha_1 \|v\|_1 + \alpha_0 \|w\|_1 + \mathcal{I}_D(r), \quad K = \begin{pmatrix} \nabla & -\text{id}_V \\ 0 & \mathcal{E} \\ W & 0 \end{pmatrix}$$

and  $D = \{r \in U \mid (r)_{\mathbf{k}} = (u_0)_{\mathbf{k}}, \text{ for all } 0 \leq \mathbf{k} < 2^{-R}N\}$ . For numerical solution of this problem, we apply a primal-dual algorithm as in [7] to the equivalent saddle point problem

$$\min_{x \in X} \max_{z \in Z} (Kx, z) - F^*(z), \quad (13)$$

with  $F^*$  the convex conjugate of  $F$ .

For this setting, the updates performed in the algorithm consist of simple arithmetic operations and the evaluation of  $(\text{id}_Z + \sigma \partial F^*)^{-1}(z)$  for  $\sigma > 0$ . By subdifferential calculus, it can be shown that this reduces to

$$(\text{id}_Z + \sigma \partial F^*)^{-1}((v, w, r)) = \begin{pmatrix} P_{\{\|\cdot\|_\infty \leq \alpha_1\}}(v) \\ P_{\{\|\cdot\|_\infty \leq \alpha_0\}}(w) \\ \text{assign}_{(u_0, \phi)}(r) \end{pmatrix},$$

where  $P_{\{\|\cdot\|_\infty \leq \lambda\}}(y)$  is a pointwise projection of  $y$  such that  $\|y\|_\infty \leq \lambda$ , with  $\|\cdot\|_\infty$  the dual norm of  $\|\cdot\|_1$ , and

$$\text{assign}_{(u_0, \phi)}(r)_{i,j} = \begin{cases} r_{i,j} - \sigma(u_0, \phi_{R,(i,j)})_2 & \text{if } 0 \leq i, j < 2^{-R}N \\ 0 & \text{else.} \end{cases}$$

Global convergence of the resulting primal dual algorithm can be assured if the stepsize parameters  $\tau, \sigma$  are such that  $\sigma\tau \leq \|K\|^{-2}$ , where  $\|K\|$  is the norm of  $K$  as linear operator from  $X$  to  $Z$ . Even though this norm can be estimated analytically, the estimate becomes quite large especially for higher levels of wavelet decomposition, i.e. for larger zooming factors. Studying the convergence proof of the algorithm in [7, Theorem 1], one can observe that it is possible to violate  $\sigma\tau\|K\|^2 < 1$  but still guarantee convergence, provided that

$$\|K(x^n - x^{n-1})\|_Z < \frac{1}{\sqrt{\sigma\tau}} \|x^n - x^{n-1}\|_X$$

is satisfied for all  $n \in \mathbb{N}$  and  $(x_n)_{n \in \mathbb{N}}$  the primal iterates. Ensuring this means to use only the span of the iterates for the estimation of  $\|K\|$ , one may hope that this allows a significantly increased stepsize. Thus we propose the following adaptive stepsize update, that allows to ensure global convergence of the primal dual algorithm:

$$\sigma_{n+1}\tau_{n+1} = S_K(\sigma_n, \tau_n) = \begin{cases} \frac{\|K(x^n - x^{n-1})\|_Z}{\|x^n - x^{n-1}\|_X} & \text{if } \theta\sigma_n\tau_n > \frac{\|K(x^n - x^{n-1})\|_Z}{\|x^n - x^{n-1}\|_X} \\ \theta\sigma_n\tau_n & \text{if } \sigma_n\tau_n > \frac{\|K(x^n - x^{n-1})\|_Z}{\|x^n - x^{n-1}\|_X} \geq \theta\sigma_n\tau_n \\ \sigma_n\tau_n & \text{if } \sigma_n\tau_n \leq \frac{\|K(x^n - x^{n-1})\|_Z}{\|x^n - x^{n-1}\|_X}. \end{cases}$$

where  $0 < \theta < 1$ . With that, the primal dual algorithm for solving the wavelet based zooming problem can be given as in Algorithm 1. The operants  $\text{div} : U^2 \rightarrow U$  and  $\text{div}_2 : U^3 \rightarrow U^2$  are defined as  $\text{div} = -\nabla^T$ ,  $\text{div}_2 = -\mathcal{E}^T$ , i.e. discrete divergence operators using backward and forward differences, respectively.

As stopping criterion we use a parameter dependent modification of the primal dual gap as in [7], denoted by  $\tilde{\mathcal{G}}$ . Provided a good parameter choice, we obtain the estimate

$$\infty > \tilde{\mathcal{G}}(x_n, z_n) \geq \alpha_1 \|\nabla u_n - v_n\|_1 + \alpha_0 \|\mathcal{E}v_n\|_1 + I_{C_n}(Wu_n) - \text{TGV}_\alpha^2(\hat{u}) \geq 0,$$

with  $x_n = (u_n, v_n)$ ,  $z_n = (p_n, q_n, w_n)$  being the iterates of Algorithm 1 and  $\hat{x} = (\hat{u}, \hat{v})$  an optimal solution of (12). Here

$$I_{C_n}(r) = \sum_{0 \leq i, j < 2^{-R}N} (C_n)_{i,j} |r_{i,j} - (u_0, \phi_{R,(i,j)})_2|,$$

with  $(C_n)_{i,j} = \gamma |(w_n)_{i,j}|$ ,  $\gamma > 1$ , incorporates data fidelity. Note that we cannot expect to get the estimate  $\tilde{\mathcal{G}}(x_n, z_n) \geq \alpha_1 \|\nabla u_n - v_n\|_1 + \alpha_0 \|\mathcal{E}v_n\|_1 - \text{TGV}_\alpha^2(\hat{u}) \geq 0$  since the iterates  $(u_n)_{n \in \mathbb{N}}$  are only contained in the data set  $U_D$  in the limit and thus it is possible that  $\alpha_1 \|\nabla u_n - v_n\|_1 + \alpha_0 \|\mathcal{E}v_n\|_1 < \text{TGV}_\alpha^2(\hat{u})$ . This was observed also in numerical experiments.

---

**Algorithm 1** Scheme of implementation for wavelet based zooming

---

```
1: function TGV-ZOOM( $u_0$ )
2:    $u \leftarrow W^{-1}(u_0)$ 
3:    $v \leftarrow 0, \bar{u} \leftarrow u, \bar{v} \leftarrow 0, p \leftarrow 0, q \leftarrow 0, w \leftarrow 0$ 
4:   choose  $\sigma, \tau > 0$ 
5:   repeat
6:      $p \leftarrow \text{proj}_{\alpha_1}(p + \sigma(\nabla \bar{u} - \bar{v}))$ 
7:      $q \leftarrow \text{proj}_{\alpha_0}(q + \sigma(\mathcal{E}(\bar{v})))$ 
8:      $w_+ \leftarrow \text{assign}_{(u_0, \phi)}(w + \sigma(W(\bar{u})))$ 
9:      $u_+ \leftarrow u - \tau(-\text{div } p + W^* w_+)$ 
10:     $v_+ \leftarrow v - \tau(-p - \text{div}_2 q)$ 
11:     $\bar{u} \leftarrow (2u_+ - u), \bar{v} \leftarrow (2v_+ - v)$ 
12:     $\sigma_+ \tau_+ \leftarrow S_K(\sigma, \tau)$ 
13:     $u \leftarrow u_+, v \leftarrow v_+, \sigma \leftarrow \sigma_+, \tau \leftarrow \tau_+$ 
14:  until Stopping criterion fulfilled
15:  return  $u_+$ 
16: end function
```

---

## 4 Numerical experiments

Now we evaluate and compare numerical results obtained with the TGV based wavelet zooming algorithm. We will see that the algorithm performs well in general and in some situations it leads to highly improved results compared to standard zooming methods. We use Algorithm 1 to obtain the high resolution reconstruction, where we initialized the adaptive stepsizes with  $\sigma = \tau = \frac{1}{3}$  and fixed the ratio between  $\alpha_0$  and  $\alpha_1$  for evaluation of the TGV functional to 4.

As stopping criterion, we require the normalized primal dual gap,  $\bar{\mathcal{G}} = \hat{\mathcal{G}}/N^2$ , to be below  $10^{-1}$  for all experiments. The purpose of using a normalized gap is to get an image size independent estimate. We tested three different wavelets, the Haar, Le Gall and CDF 9/7 wavelet as described in Section 2. For the Haar wavelet, due to orthogonality, we used a simplified version of the algorithm, similar to a the JPEG decompression algorithm presented in [2].

We first consider a four times magnification of a patch of the Barbara image, containing a stripe structure. For better comparability, we used the original image rather than a downsampled version. Thus the downsampling procedure is not known and cannot favor any particular method, but also no ground truth is available. The results, using the three different wavelet types as well as interpolation with a Lanczos 2 [11] filter, are shown in Figure 1. As one can see, the linear filter based zooming leads to blurring of the stripes while our method yields a reconstruction appearing much sharper. Using the CDF 9/7 wavelets results in the best reconstruction quality. In particular, we observe that not only the edges are preserved, but also the geometrical information is extended in a natural manner for the CDF 9/7 wavelet (as opposed to the Haar wavelet, where “geometrical staircasing” occurs).

Next, Figure 2 shows results of the TGV based zooming method for the CDF 9/7 wavelet in the situation where the subsampling process is known and fits to the model assumption, i.e. the subsampling was done by applying a wavelet decomposition on the original image and neglecting the high resolution detail coefficients. On the left of the figure, we show the subsampled version of the image and its upsampling by setting the unknown detail coefficients to zero. This is the initial image for our TGV based method. On the right, we show the outcome of our method as the primal dual gap is below  $10^{-1}$ . With that we compare the effect of TGV regularization independent of the wavelet basis. As one can see, indeed the reconstruction quality is clearly improved when TGV based regularization is applied, which justifies the application of TGV regularization instead of simple wavelet based upsampling. This is reflected also by an improved *Peak Signal to Noise Ratio* (PSNR) of the mean-value corrected images: The TGV based reconstruction yields a PSNR of 29.70 while the wavelet upsampling yields 29.27. The PSNR is also highly increased with respect to standard interpolation methods (Pixel repetition: 25.06, Cubic: 26.13, Lanczos 2: 26.13), however, this must be partly explained by the downsampling being done accordance with the wavelet model.

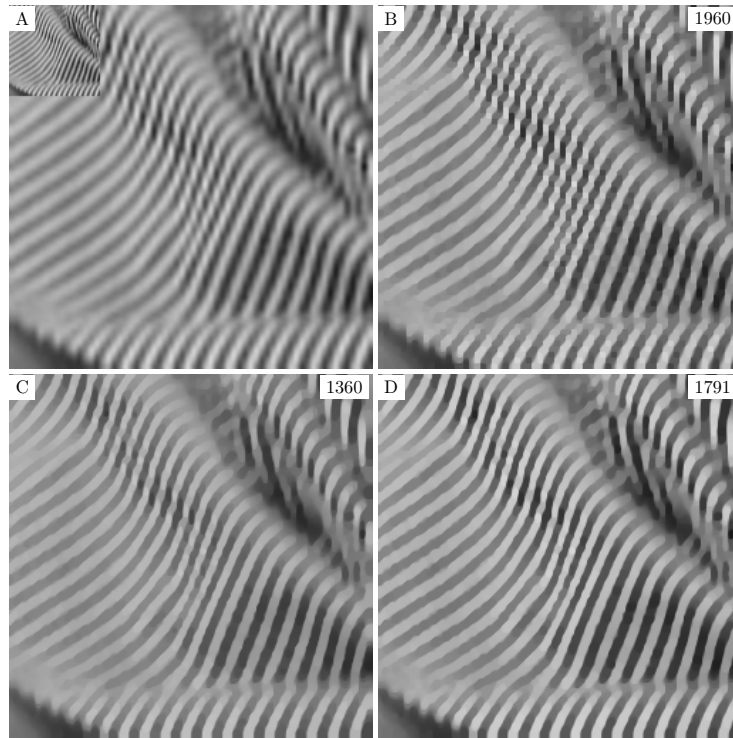


Fig. 1: A: 4 times magnification by Lanczos 2 filtering. B-D: 4 times magnification by TGV based wavelet zooming using the Haar, Le Gall and CDF 9/7 wavelet, with iteration number on top right. The stopping rule was  $\overline{\mathcal{G}}(x_n, z_n) < 10^{-1}$ .

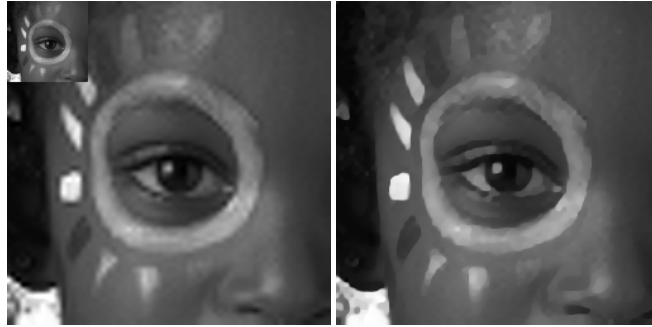


Fig. 2: Girls-eye image ( $256 \times 256$  pixels). Left: CDF 9/7-Wavelet down- and upsampled image (without TGV regularization). Right: TGV based wavelet upsampling using CDF 9/7 wavelet. The stopping rule was  $\bar{\mathcal{G}}(x_n, z_n) < 10^{-1}$ .

## References

1. K. Bredies. Recovering piecewise smooth multichannel images by minimization of convex functionals with total generalized variation penalty. SFB Report 2012-006. <http://math.uni-graz.at/mobis/publications.html>.
2. K. Bredies and M. Holler. Artifact-free decompression and zooming of JPEG compressed images with total generalized variation. In *CCIS*, volume 359. Springer, 2012. To appear.
3. K. Bredies, K. Kunisch, and T. Pock. Total generalized variation. *SIAM J. Imag. Sci.*, 3(3):492–526, 2010.
4. K. Bredies, K. Kunisch, and T. Valkonen. Properties of  $L^1 - \text{TGV}^2$ : The one-dimensional case. *J. Math. Anal. Appl.*, 389(1):438–454, 2013.
5. K. Bredies and T. Valkonen. Inverse problems with second-order total generalized variation constraints. In *Proceedings of SampTA*, Singapore, 2011.
6. A. Chambolle. An algorithm for total variation minimization and applications. *J. Math. Imaging Vis.*, 20:88–97, 2004.
7. A. Chambolle and T. Pock. A first-order primal-dual algorithm for convex problems with applications to imaging. *J. Math. Imaging Vis.*, 40:120–145, 2011.
8. A. Cohen, I. Daubechies, and J.-C. Feauveau. Biorthogonal bases of compactly supported wavelets. *Commun. Pur. Appl. Math.*, 45(5):485–560, 1992.
9. A. Cohen, I. Daubechies, and P. Vial. Wavelets on the interval and fast wavelet transforms. *Appl. Comput. Harmon. Anal.*, 1(1):54 – 81, 1993.
10. I. Daubechies. *Ten Lectures on Wavelets*. Number 61 in CBMS-NSF Lecture Notes. SIAM, 1992.
11. C. E. Duchon. Lanczos Filtering in One and Two Dimensions. *J. Appl. Meteor.*, 18(8):1016–1022, 1979.
12. N. Kaulgud and U. B. Desai. Image zooming: Use of wavelets. In *The International Series in Engineering and Computer Science*, volume 632, pages 21–44. Springer, 2002.
13. F. Malgouyres and F. Guichard. Edge direction preserving image zooming: A mathematical and numerical analysis. *SIAM J. Numer. Anal.*, 39:1–37, 2001.
14. R. M. Young. *An Introduction to Nonharmonic Fourier Series*. Academic Press, 2001.
15. X. Zhang and T. F. Chan. Wavelet inpainting by nonlocal total variation. *Inverse Probl. Imag.*, 4:191–210, 2010.